Int J Thermophys (2009) 30:1106–1117
DOI 10.1007/s10765-009-0557-7

Sound-Speed Sensor for Gas Pipeline Applications

L. Ruffine · J. P. M. Trusler

Received: 14 October 2008 / Accepted: 9 January 2009 / Published online: 29 January 2009

Abstract A sensor, based on a small cylindrical acoustic resonator that may be suitable for measuring the speed of sound in natural and other process gases under pipeline conditions is described. The resonator is physically robust and requires minimal calibration. The speed of sound is obtained from the resonance frequency of a single longitudinal mode of oscillation that is isolated in the frequency spectrum of the cavity and can therefore be located and measured automatically. The design and acoustic model of the sensor are discussed. The performance of a prototype device was validated by means of measurements on three pure gases: argon, nitrogen and methane. The results of these measurements agree with the predictions of the most accurate equations of state with an absolute average deviation of about 0.02 % and a maximum absolute deviation of 0.06 % at temperatures between 293.15 K and 333.15 K and at pressures between 0.1 MPa and 10 MPa. Additional design features have been tested that may facilitate the deployment of the sensor in a pipeline system by: (a) preventing problems with condensate when operating near or below the dew temperature and (b) ensuring that the sensor is filled with a representative sample of the pipeline gas. Finally, we discuss how the design methodology may be applied to optimize the sensor dimensions for different operating conditions, such as high or low gas pressure.

Keywords Acoustic resonator · Argon · Methane · Natural gas · Nitrogen · Pipeline · Speed of sound

L. Ruffine · J. P. M. Trusler (✉)
Department of Chemical Engineering, Imperial College London,
South Kensington Campus,
London SW7 2AZ, UK
e-mail: m.trusler@imperial.ac.uk

1 Introduction

Physicochemical properties of pipeline natural gases, both pre- and post-processing, are of significant technical and economic importance. These properties of course depend upon the composition of the gas and, with globalization of supply and comingling of streams, the composition and quality of natural gases in pipeline transmission systems are increasingly variable. On-line composition measurements, e.g., by gas chromatography, may be used to determine many of the properties of interest but this approach is costly to implement and maintain. Consequently, there is interest in developing robust sensors to provide information on key thermophysical properties, possibly by indirect means such as inference.

As a result of research carried out over the past 20 years, systems have been developed to evaluate the calorific value [1], hydrate formation conditions [2], and dew point [3] of natural gases from measurements of a few physicochemical properties. Among such properties, the speed of sound is particularly interesting from both the economical and technical points of view. For example, the speed of sound is sensitive to gas composition and may be measured with high accuracy, low cost, and fast response time.

In this paper, we describe the design and validation of a robust speed-of-sound sensor that is suitable for gas-pipeline applications. The objective of the design process was to develop a low-cost and robust sensor, suitable for permanent deployment in a pipeline system, and to be able to provide reliable measurements over wide ranges of temperature and pressure. The application of the sensor to the pipeline environment involves taking into consideration several technical issues linked with the sampling conditions. In this present study, we consider some of the issues and test possible solutions.

Low-frequency acoustic resonators have been widely recognized as reliable laboratory instruments for highly accurate measurements of the speed of sound. Spherical [4] and cylindrical cavities [5–7] in particular have received much attention. In the present case, the simplicity and flexibility of the cylindrical geometry are advantageous.

2 Design of the Sensor

As illustrated in Fig. 1, the sensor was a thick-walled cylindrical acoustic cavity resonator provided with a number of vent holes in the wall which permitted the interior to fill with the surrounding gas. The entire sensor was designed to be immersed in the gas, either in the main pipeline or on a by-pass branch, and to be operated over the full range of temperatures and pressures encountered in pipeline operations.

The end plates of the cavity resonator served as electro-acoustic transducers and were used to excite and detect resonance of the gas contained within. The basis of the measurement was determination of the resonance frequency of the second longitudinal mode of oscillation which is related to the speed of sound in the gas in a very simple way. When driven by an associated electronics package, it was possible to measure the resonance frequency of this and other modes of oscillation with an uncertainty smaller then 0.01 %.

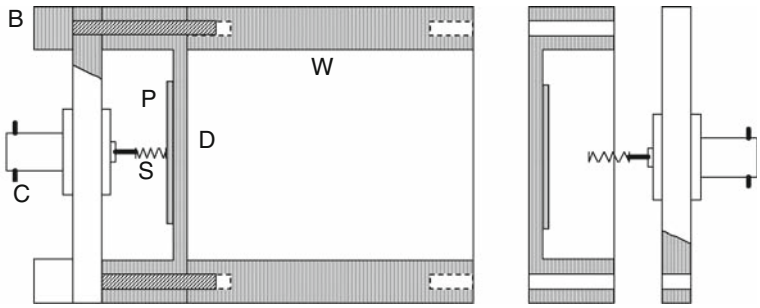

Fig. 1 Partial cross section of the acoustic resonator. B, bolt; C, coaxial connector; D, diaphragm; P, piezoelectric-ceramic disc; S, spring contact; W, wall of cylinder

The prototype sensor was fabricated from Type-316 stainless-steel barstock. The cylinder was of length 20 mm, internal diameter 15 mm, and wall thickness 3 mm. It was provided with four axial tapped holes in each end, which permitted attachment of the end-plate transducer units, and with eight 1 mm diameter radial holes for the purpose of filling.

Each end-plate transducer unit took the form of a Type-316 stainless-steel cylinder, of diameter 21 mm and length 20 mm, which was counter-bored axially from the rear face to produce a stiff diaphragm of diameter 15 mm and thickness approximately 1.1 mm. A shallow (approximately 0.1 mm deep) concentric recess was machined in the rear face of the diaphragm to permit location of a piezoelectric disc. The piezoelectric disc (PZT, 10 mm diameter $\times$ 0.4 mm thick, poled axially and nickel-plated on the major faces) was bonded to the diaphragm with a thin layer of epoxy resin. By placing the joint under compression while the resin cured, electrical contact was maintained between the metallic diaphragm and the adjoining electrode on the disc. A cover plate, fitted with a bulkhead SMA co-axial connector, closed the rear, and a small spring was used to make electrical contact with the rear electrode of the PZT. A similar transducer design was reported by Ewing et al. [8].

The length-to-diameter ratio of the cavity resonator was chosen such that the second longitudinal mode of oscillation was isolated in the frequency spectrum, avoiding interference with both the fundamental radial mode and compound modes of oscillation. The second longitudinal mode was preferred over the fundamental because, on symmetry grounds, it does not couple with translational oscillations of the cavity itself. Modes of oscillation involving angular (azimuthal) excitation should not be excited with our axisymmetric transducer arrangement but the chosen aspect ratio clearly separates these modes too from the longitudinal resonance of interest. These criteria were met by the 4/3 length-to-diameter ratio adopted.

The stainless-steel diaphragm and attached PZT disc formed a reversible flexure-mode electro-acoustic transducer with sufficient sensitivity to drive and detect sound waves in gases at pressures as low as 0.1 MPa. In designing the transducer, we modeled the diaphragm as an un-tensioned edge-clamped homogeneous circular plate of uniform thickness and took account of the theoretical fundamental resonance

frequency f_1 and the mean compliance in the limit of zero frequency C. These quantities are given by [9]

$$f_1 = \nu_1^2 \left(d/4\pi b^2\right) \left[E/\left\{3\rho_s \left(1-\sigma^2\right)\right\}\right]^{1/2} \quad (1)$$

$$C = \left(1-\sigma^2\right) b^4/\left(16Ed^3\right), \quad (2)$$

where $\nu_1 = 1.015\pi$ is an eigenvalue, b is the radius (equal to the cavity radius in the present case), d is the thickness, E is Young's modulus, σ is Poisson's ratio, and ρ_s is the density of the diaphragm material. Here, C is defined as the mean surface displacement divided by the mean excess pressure imposed on one face. In order to avoid over coupling and to ensure an approximately flat frequency response in the range of interest, the fundamental resonance frequency of the flexure transducer was designed to be well above the operating frequency of the cavity. The transducers were further required to offer adequate sensitivity but at the same time, to be sufficiently stiff to avoid perturbing the cavity resonances excessively. To assess this second criterion, we used acoustic perturbation theory to calculate the shift Δf_{end} in the frequency of a longitudinal cavity resonance resulting from the non-zero compliance. At frequencies below f_1, this is given in a lumped-circuit approximation by

$$\Delta f_{\text{end}}/f = -\rho u^2 (C/L) \left[1 - (f/f_1)^2\right] \quad (3)$$

where ρ is the gas density, u is the speed of sound in the gas, and L is the length of the cylindrical cavity [9]. With $d = 1.1\,\text{mm}$ and $b = 7.5\,\text{mm}$, the theoretical resonance frequency and mean static compliance of the stainless-steel diaphragm were $f_1 = 49\,\text{kHz}$ and $C = 6.9 \times 10^{-13}\,\text{m} \cdot \text{Pa}^{-1}$. This gives $\Delta f_{\text{end}}/f < 10^{-3}$ at the maximum operating pressure in typical gases, which is adequately small. We do not expect f_1 and C to conform exactly to Eqs. 1 and 2, especially in the presence of the PZT, but Eq. 3 should be a good approximation provided that C and f_1 are determined experimentally. Clearly these equations, together with appropriate criteria for f_1 and the maximum value of $(\Delta f_{\text{end}}/f)$, would permit the selection of alternative diaphragm dimensions suitable for operation in other pressure regimes.

3 Test Facility

For purposes of testing, the resonator was mounted inside a 'spool-piece' pressure vessel comprising a section of 50 mm nominal diameter stainless-steel pipe fitted with industry-standard weld-neck flanges (DN50/PN100 rating), each closed by a blanking plate, sealed with a Novus Type 34 gasket, and retained by four 24 mm diameter high-tensile steel bolts. This vessel was suitable for a maximum working pressure of 10 MPa. The upper end plate of the vessel was fitted with a pair of welded and hermetically-sealed BNC coaxial electrical feedthroughs (Ceramaseal Model 7007-02-W) and four 3.2 mm NPT-threaded ports. Of these four threaded ports, two were fitted with compression-sealed four-wire electrical feedthroughs (Conax MHC series), one was

used for evacuation and filling with gas, and the fourth was connected to the pressure transducer. The BNC feedthroughs were each fitted with a female SMA adapter on the inside of the vessel and connected to the opposite ends of the resonator by means of semi-rigid coaxial cables with SMA plugs. The pressure vessel was immersed in a temperature-controlled water bath regulated to ±0.05 K.

The pressure was measured by means of a quartz transducer (Paroscientific Digiquartz Model 43K-101) with a full-scale range of 21 MPa and an uncertainty of less than 2 kPa. The temperature of the cavity was measured with a four-wire thin-film platinum resistance thermometer (Minco Model S651) that was bonded to the outer cylindrical surface of the resonator and connected to an external AC resistance bridge (ASL Model F17A) by means of wires passing through one of the Connax fittings. The thermometer was calibrated in situ by comparison with a conventional platinum resistance thermometer probe inserted through one of the open fluid ports, and the estimated uncertainty of the temperature was 0.05 K. During some of the experiments, a pair of polyimide-insulated flexible heaters were also bonded to the exterior of the resonator and connected to an external DC power supply (Thurlby-Tander Model TSX 3510P) by means of wires passing through the other Conax fitting.

For measurement of the resonance frequencies of the gas-filled cavity, one electro-acoustic transducer was connected to a sine-wave function generator (Hewlett-Packard HP3325B) and driven at an amplitude of approximately 1 V peak-to-peak. The second electro-acoustic transducer then served as a detector and it was connected to the input of a two-phase lock-in amplifier (Stanford SRS530) operating at the driving frequency. Resonance frequencies and half-widths were determined by analysis of measurements of the in-phase and quadrature components of the detected voltage at a set of discrete values of driving frequency spanning the resonance of interest [4]. This method of measurement permitted the resonance frequency to be determined with an uncertainty much smaller than 0.01 % with a measurement time of approximately 30 s. Since the two transducers were interchangeable, it made no difference which was selected as the drive unit.

4 Acoustic Model

The speed of sound u in the gas was obtained from the resonance frequency f_{200} of the second longitudinal mode of oscillation. In an idealized resonator with rigid walls and in the absence of viscous- and thermal-boundary-layer effects, the wavelength of the sound in this mode of oscillation is exactly equal to the length L of the cavity, so that $u = f_{200}\, L$. In a real cavity, corrections have to be made such that the speed of sound u is given by

$$u = (f_{200} - \Delta f)\, L, \tag{4}$$

where Δf is the sum of two correction terms as follows:

$$\Delta f = 2\Delta f_{\mathrm{end}} + \Delta f_{\mathrm{v-t}}. \tag{5}$$

The first of these terms have already been discussed (the prefactor 2 arises from the presence of two identical end plates). The second term in Eq. 5, $\Delta f_{\mathrm{v-t}}$, represents the effects of the viscous and thermal boundary layers in the gas at the walls of the cavity and is given by [9,10]

$$\Delta f_{\mathrm{v-t}} = -\frac{1}{2} f_{200} \left[1.75\,(\gamma - 1)\, D_{\mathrm{t}}^{1/2} + D_{\mathrm{v}}^{1/2} \right] / \left(\pi f_{200} b^2 \right)^{1/2}, \tag{6}$$

where γ, D_{t}, and D_{v} are properties of the gas as follows:

$$\gamma = C_{p,\mathrm{m}} / C_{V,\mathrm{m}}, \tag{7}$$

$$D_{\mathrm{t}} = \lambda M / \left(\rho C_{p,\mathrm{m}} \right), \tag{8}$$

$$D_{\mathrm{v}} = \eta / \rho. \tag{9}$$

Here, $C_{p,\mathrm{m}}$ is the isobaric molar heat capacity, $C_{V,\mathrm{m}}$ is the isochoric molar heat capacity, D_{t} is the thermal diffusivity, λ is the thermal conductivity, M is the molar mass, ρ is the density, D_{v} is the viscous diffusivity, and η is the shear viscosity.

The presence of the filling holes in the wall of the cavity also gives rise to a perturbation which, in principle, should be accounted for by a third contribution to Δf. However, we chose to place the holes at a distance of $L/4$ from an end of the cavity where, the unperturbed wavefunction is zero. Accordingly, the effect of a small hole centered on such a location is identically zero on symmetry grounds. We do not expect this to apply for large holes because of the non-linear variation of the wavefunction with the axial coordinate. However, in leading order, the effect of holes in the cavity wall is independent of the properties of the gas leading to a correction that is a constant fraction of the resonance frequency. In that case, the effect (if any) of the filling holes would be absorbed in an effective value of the pathlength L obtained by calibration.

The combined corrections are not large under any condition in the working range of the sensor, with typically $|\Delta f|/f_{200} < 2 \times 10^{-3}$. The relative visco-therm correction, $\Delta f_{\mathrm{v-t}}/f_{200}$, varies like $\rho^{-1/2}$ and is therefore important at low pressures, while the relative end correction varies like ρ and is therefore important at high pressures. Since the corrections are small, one could simply neglect them and accept errors of the order of 0.2 %. A better and only slightly more demanding approach is to use approximate values of the various thermophysical properties of the gas that appear in the acoustic model. Specifically, we advocate approximating all of the thermodynamic properties which appear by their perfect-gas values and replacing the two transport properties by the corresponding values for the dilute gas:

$$\gamma = C_{p,\mathrm{m}}^{\mathrm{pg}} / \left(C_{p,\mathrm{m}}^{\mathrm{pg}} - R \right), \tag{10}$$

$$D_{\mathrm{t}} = \lambda_0 RT / \left(p C_{p,\mathrm{m}}^{\mathrm{pg}} \right), \tag{11}$$

$$D_{\mathrm{v}} = \eta_0 RT / (Mp). \tag{12}$$

Here, $C_{p,\mathrm{m}}^{\mathrm{pg}}$ is the perfect-gas isobaric molar heat capacity of the gas, and subscript '0' denotes dilute-gas values of the thermal conductivity and viscosity. These quantities depend only upon temperature and composition; they are known accurately

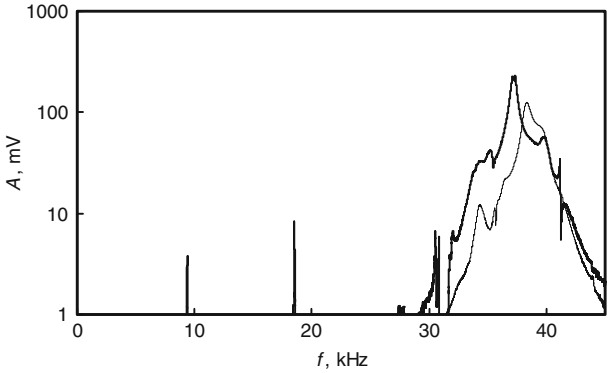

Fig. 2 Frequency response of the acoustic cavity at $T = 313\,\mathrm{K}$: – – –, nitrogen filled at $p = 5\,\mathrm{MPa}$; ____, vacuum

for most pure gases and may be estimated reliably for gas mixtures. Under the same assumptions, the end correction is

$$\Delta f_{\mathrm{end}}/f_{200} = -\gamma p\,(C/L)\,/\left[1-(f_{200}/f_1)^2\right]. \tag{13}$$

The values of the thermophysical properties used in this study for the calculation of the corrections terms were obtained as follows: for argon, $C^{\mathrm{pg}}_{p,\mathrm{m}} = 2.5\,R$, λ was from Perkins et al. [11], and η was from Younglove and Hanley [12]; for nitrogen, $C^{\mathrm{pg}}_{p,\mathrm{m}} = 3.5\,R$ and the transport properties were from Younglove [13]; finally, for methane, $C^{\mathrm{pg}}_{p,\mathrm{m}}$ was from Setzmann and Wagner [14], λ was from Friend et al. [15], and η was from Younglove and Ely [16]. The smallness of the corrections is such that properties accurate to $\pm 20\,\%$ are sufficient to permit sound-speed measurements with an uncertainty of $0.05\,\%$. Accordingly, many natural gases with high methane content could be treated as pure methane for the purposes of estimating Δf [5]. Alternatively, a rough compositional analysis may be combined with available techniques for estimating the desired thermophysical properties of gas mixtures for the purpose of calculating the corrections.

5 Experimental Results

The gases used in this study (argon, nitrogen, and methane) were supplied by BOC. The argon and nitrogen were high-purity gases with a claimed purity of 99.9999 mol%. The methane supplied was technical-grade gas with a specified minimum purity of 99.5 mol%. According to the manufacturers, the main impurities were other light hydrocarbons ($\leq$0.3 mol%), nitrogen ($\leq$0.1 mol%), oxygen ($\leq$0.001 mol%), and water ($\leq$0.001 mol%). A few additional measurements were also made in a sample of higher-purity methane sourced from Linde for which the claimed purity was 99.95 mol%. All gases were used without further purification.

Figure 2 shows spectra of the acoustic cavity, recorded both under vacuum and when filled with nitrogen at $p = 5\,\text{MPa}$ and $T = 313\,\text{K}$ Even under vacuum, a signal was obtained at the detector transducer, presumably as a result of sound transmission through the cavity wall. We attribute the major peak in the vacuum spectrum to the fundamental resonances of the transducers at $f_1 = 39\,\text{kHz}$, considerably lower than the theoretical value of 49 kHz for the edge-clamped plate in the absence of the PZT. The signal in the presence of gas showed clear peaks at the first and second longitudinal resonance modes superimposed on a very small background signal at $f < 25\,\text{kHz}$. The maximum occurred at a frequency close to the expected resonance of the fourth longitudinal mode which, being close to the fundamental frequency of the transducers, was excited with great efficiency. The amplitude of the signal resulting from resonances in the gas varied rapidly with pressure while the background signal transmitted through the cavity wall did not. At the lowest pressure considered here, $p = 0.1\,\text{MPa}$, the resonance signal of interest was approximately equal to the background. However, the method used to analyze the resonance data accounted explicitly for the background and the resonance frequencies f_{200} and half-widths g_{200} could be measured with a precision of at least $0.01\,g_{200}$ under all conditions studied. Since the quality factor, $Q = f_{200}/(2g_{200})$, was >200, the resonance frequencies were always obtained with a precision of at least 0.01 %.

The pathlength of the cavity L and the mean static compliance of the transducer C were obtained from an isothermal calibration in a reference gas of known sound-speed: one point at low pressure and one at high pressure, the latter sensitive to C and the former not. This calibration was carried out in argon at $T = 333\,\text{K}$ and at pressures of 0.5 MPa and 10 MPa; the speeds of sound at these state points were obtained from the equation of state of Tegeler et al. [17] with an uncertainty of <0.02 %. The pathlength was obtained at other temperatures assuming a linear relationship,

$$L(T) = L_0\{1 + \alpha(T - T_0)\}, \tag{14}$$

with $\alpha = 18 \times 10^{-6}\,\text{K}^{-1}$ [18].

The 'baseline' sensor was tested extensively in measurements on the three test gases at three temperatures between 293 K and 333 K and at pressures up to approximately 10 MPa. In these tests, the resonance frequency f_{200} varied between about 16 kHz and 23 kHz, while the quality factor Q was between 200 and 1,000. Figures 3, 4, and 5 show the results of these test measurements and of comparisons between the measured speeds of sound and the predictions of the most accurate equations of state available for argon [17], nitrogen [19], and methane [14]. For argon and nitrogen, the agreement is mostly within ±0.02 %. There is a tendency for the deviations to increase at low pressures reaching, in the worst case, +0.04 % for nitrogen at $T = 293\,\text{K}$ and $p = 0.15\,\text{MPa}$. Of course, the good agreement for argon is due in part to the fact that two points were used for sensor calibration. In the case of nitrogen, the results have a positive mean deviation (bias) of about 0.02 %. The results for technical grade methane are slightly less good with a bias of −0.04 % but the worst deviation is still only −0.06 %. The relatively less good results for methane may have been partly the result of impurities. Nevertheless, the results clearly indicate that the sensor can be used to measure the speed of sound with an error of less than 0.1 %. We did not test

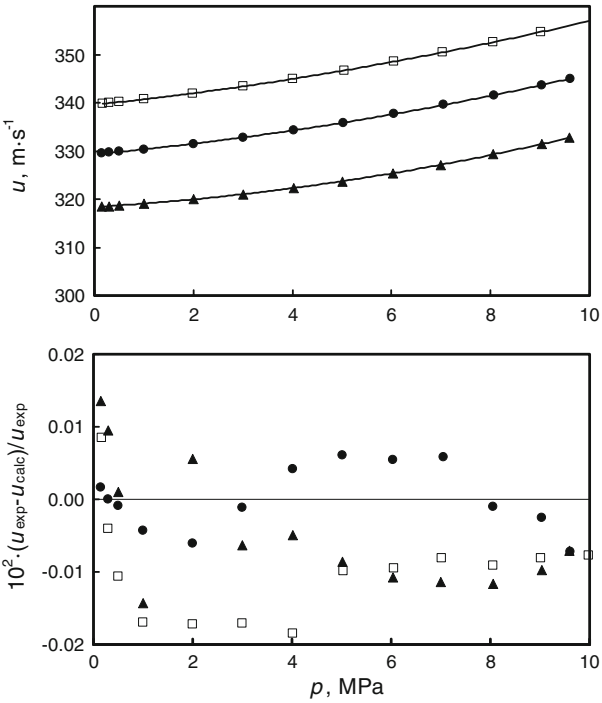

Fig. 3 Speed of sound u in argon as a function of the pressure in comparison with values calculated from the equation of state of Tegeler et al. [17]: □, $T = 332.45$ K; ●, $T = 312.82$ K; ▲, $T = 292.19$ K; _____, Tegeler et al. [17]

the device with gas mixtures, first, because it is difficult to determine the composition accurately and, second, because of lower confidence in the accuracy of the available equations of state for mixtures.

A few additional measurements were also made with a second sensor of identical design. In this case, the pathlength was calibrated in a single-point measurement on nitrogen at $T = 306$ K and $p = 0.2$ MPa, while the compliance parameter C was assumed to be identical to that obtained for the first sensor. Measurements were then made on methane of claimed minimum purity 99.95 % at $T = 306$ K and at pressures of 2 MPa, 5 MPa, and 10 MPa. In this case, the measured speeds of sound agreed with the equation of state of Setzmann and Wagner [14] to be within ±0.02 %. These data suggest that the slightly poorer results obtained for the technical grade methane may be attributed to its lower purity. They also demonstrate that the compliance parameter C is transferrable between sensors of identical construction.

6 Issues Related to Pipeline Deployment

Although we have tested the sensor only in static gas, we have considered some of the issues that would arise in pipeline deployment. The sensor must be filled with a representative sample of the pipeline gas, operated at a known and preferably controlled

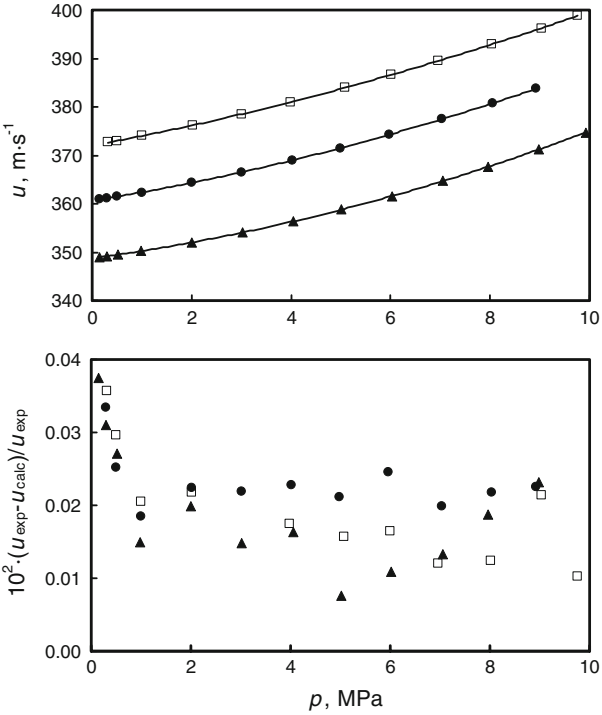

Fig. 4 Speed of sound u in nitrogen as a function of the pressure in comparison with values calculated from the equation of state of Span et al. [19]: □, $T = 332.45\,\mathrm{K}$; •, $T = 312.82\,\mathrm{K}$; ▲, $T = 292.19\,\mathrm{K}$; _____, Span et al. [19]

temperature, and protected from erosion, corrosion, particle ingress, and condensation. There is also the question of interference from ambient noise to consider.

The sensor might be installed directly in the pipeline, but this may not be desirable on a large-diameter gas transmission line. A more promising situation would be to install the sensor in a parallel branch supplied with a bleed flow from the main pipeline. Such a branch could be protected from particle ingress with filters and provide an environment in which the sensor might be easily temperature regulated.

The provision of a temperature regulation system would permit the device to be operated at an elevated temperature thereby both reducing the probability of condensation within the cavity and accelerating the evaporation of any condensate that might be washed into the cavity. However, one concern (especially in sub-sea installations) is the power requirements of such a system. In order to quantify both the impact of local heating on the sensor accuracy and the power requirements, we have implemented a simple direct electric heating scheme, with a pair of low-voltage polyimide-insulted etched-foil heater elements bonded to the outer wall of the cavity. Tests in nitrogen at $p = 10\,\mathrm{MPa}$ showed that the ratio of power dissipation to temperature rise was approximately $0.5\,\mathrm{W}\cdot\mathrm{K}^{-1}$, so that power requirements are very modest. Operating with a temperature rise of about 5 K, the impact on the accuracy of the measured sound-speed was found to be $<0.05\,\%$ under all conditions investigated provided that

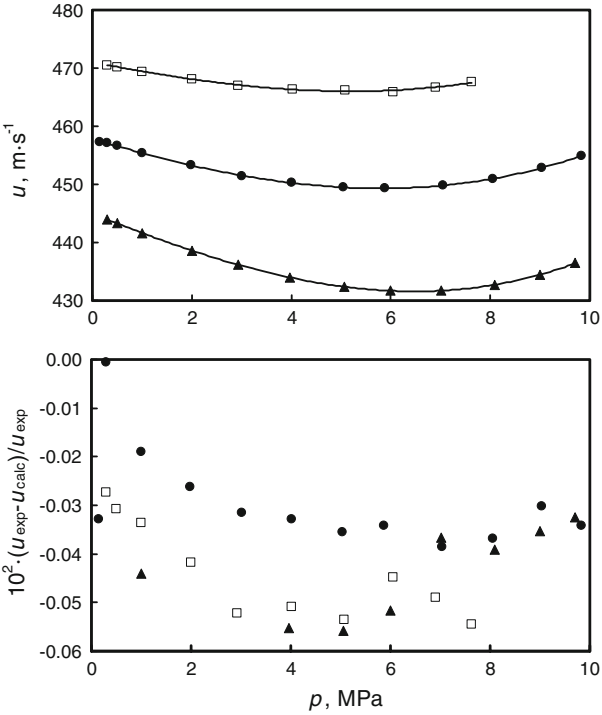

Fig. 5 Speed of sound u in methane as a function of the pressure in comparison with values calculated from the equation of state of Setzmann and Wagner [14]: □, $T = 332.45$ K; •, $T = 312.82$ K; ▲, $T = 292.19$ K; _____, Setzmann and Wagner [14]

the data were associated with the measured temperature of the cavity wall. In these tests, the heaters were operated at various fixed currents, without feedback control of the temperature, and the time required to attain thermal equilibrium after a change in current was approximately 20 min. We expect that a much faster response time could be achieved with active control of the sensor's temperature.

In the present design, the cavity was not sealed and gas entered through openings in the cylindrical wall. Simply immersing the sensor in a flow may be sufficient to ensure that the cavity contains a representative sample provided that holes are sufficiently large. In the baseline sensor, these holes were of 1 mm diameter. However, we have also tested the effects of increasing the size of the filling holes. The holes were increased to 3 mm diameter for the first 1 mm, and then expanded to 8 mm diameter for the remaining 2 mm of the wall thickness. The effect of these enlarged holes was to increase the resonance frequency of the cavity by a constant fraction of 0.5 %. This is entirely absorbed into the effective pathlength when L is determined by calibration. For example, after recalibration, speeds of sound measured in nitrogen along the isotherm at $T = 333$ K remained in the same close agreement with the equation of state of Span et al. [19] as found with the baseline sensor. Increasing the size of the smaller diameter to 5 mm, resulted in a larger shift of approximately 2.8 % relative to the baseline sensor.

7 Conclusion

The approach advocated in this work, incorporated several key ideas in an advantageous way. First, we optimize the cavity geometry to isolate one easy-to-measure acoustic resonance and focus on that mode. Second, we employ robust and reliable wide-band piezoelectric transducers that provide adequate signals over a 100 to 1 range of gas pressure. Third, we employ an acoustic model of the sensor that treats these transducers explicitly and that allows the thickness of the diaphragm to be matched to the desired pressure range. Fourth, we advocate simple approximations for the physical properties required in the application of the acoustic model. Finally, our approach permits a single-point calibration of production sensors.

The practical implementation of the sensor described in this article is suitable for sound-speed measurements in pipeline gases at pressures up to 10 MPa. The sensor was robust, of simple construction, and easy to use. A comparison of the measured speeds of sound with values calculated from reference-quality equations of state demonstrate an uncertainty of about 0.05 %. This is comparable to the accuracy claimed by Younglove and Frederick [5] at similar temperature and pressure conditions, but not as good as the ±0.01 % claimed by Hurly [7]. Finally, laboratory tests have demonstrated that the instrument can fulfil several of the requirements for pipeline application.

Acknowledgments This work was supported by grants from the Department of Trade and Industry (Grant number TP/2/SC/6/l/10244), Schlumberger Cambridge Research, and the Royal Academy of Engineering.

References

1. M. Jaeschke, P. Schley, R. Van Rosmalen, Int. J. Thermophys. **23**, 1013 (2002)
2. A.A. Elgibaly, A.M. Alkamel, Fluid Phase Equilib. **152**, 23 (1998)
3. S.Z. Akhtar, Hydrocarb. Process. **84**, 94 (2005)
4. M.R. Moldover, J.B. Mehl, M. Greenspan, J. Acoust. Soc. Am. **79**, 253 (1986)
5. B.A. Younglove, N.V. Frederick, Int. J. Thermophys. **11**, 897 (1990)
6. F.W. Giacobbe, J. Acoust. Soc. Am. **94**, 1200 (1993)
7. J.J. Hurly, Int. J. Thermophys. **20**, 455 (1999)
8. M.B. Ewing, M.L. McGlashan, J.P.M. Trusler, J. Chem. Thermodyn. **17**, 549-559 (1985)
9. J.P.M. Trusler, *Physical Acoustics and Metrology of Fluids* (Adam Hilger, Bristol, 1991)
10. K.A. Gillis, M.R. Moldover, A.R.H. Goodwin, Rev. Sci. Instrum. **62**, 2213 (1991)
11. R.A. Perkins, D.G. Friend, H.M. Roder, C.A. Nieto de Castro, Int. J. Thermophys. **12**, 965 (1991)
12. B.A. Younglove, H.J.M. Hanley, J. Phys. Chem. Ref. Data **15**, 1323 (1986)
13. B.A. Younglove, J. Phys. Chem. Ref. Data **11**, 1 (1982)
14. U. Setzmann, W. Wagner, J. Phys. Chem. Ref. Data **20**, 1061 (1991)
15. D.G. Friend, J.F. Ely, H. Ingham, J. Phys. Chem. Ref. Data **18**, 583 (1989)
16. B.A. Younglove, J.F. Ely, J. Phys. Chem. Ref. Data **16**, 577 (1987)
17. C. Tegeler, R. Span, W. Wagner, J. Phys. Chem. Data **28**, 779 (1999)
18. *CRC Handbook of Chemistry and Physics*, 87th edn, ed. by D.R. Lide (Taylor & Francis, London, 2006)
19. R. Span, E.W. Lemmon, R.T. Jacobsen, W. Wagner, A. Yokozeki, J. Phys. Chem. Data **29**, 1361 (2000)